forum acusticum 2023

ON-FIELD MEASUREMENT FOR sUAS NOISE CHARACTERISATION

Carlos Ramos-Romero[1*] **Nathan Green**[1]
César Asensio[2] **Antonio J Torija**[1]

[1] Acoustics Research Centre, University of Salford, Manchester M5 4WT, UK.
[2] Instrumentation and Applied Acoustics research group (I2A2),
Universidad Politécnica de Madrid, Madrid 28031, Spain.

ABSTRACT

With the imminent introduction of multi-rotor aircraft systems in airspace and the expectation of their operation near urban areas, noise emissions from this new type of noise sources have become an important research topic, mainly because they have been reported to be more annoying than other conventional urban noise sources(*e.g.,* road vehicles) at the same loudness level.

Specific techniques for adequately measuring sound produced by small Unmanned Aircraft Systems (sUAS) are currently being developed by international standardisation organisations, aviation agencies, and research institutions. All of these efforts are intended to be relevant in establishing common measurement protocols between environmental policymakers, stakeholders, drone companies, and academia.

This paper presents a multichannel on-field methodology for the characterisation of sUAS noise. In addition to the measurement procedure, the methodology covers the back-propagation techniques applied in the analysis of each microphone recording, and preliminary results, which include acoustic metrics (L_{Amax}, L_{Aeq} and L_{AE}), directivity plots, and noise hemispheres during flyovers, presented in both the time and frequency domains.

Keywords: *sUAS noise, on-field noise measurements, noise metrics, directivity, noise hemispheres*

**Corresponding author*: C.A.RamosRomero@salford.ac.uk.

1. INTRODUCTION

The literature has reported experimental protocols for the small Unmanned Aircraft Systems (sUAS) noise measurement under controlled indoor and semi-controlled outdoor conditions. [1–3]. Although realistic flight operations within anechoic chambers may be restricted by the size of the facilities, outdoor experiments must cope with not always favourable environmental conditions and background noise.

To guarantee objective and repeatable measurements of sUAS noise outdoors, a number of techniques and configurations have been proposed in recent years, where arrays of microphones mounted on a reflective ground plate are the most common measurement setup [4].

Regarding noise metrics, recent *"Guidelines for Noise Measurement of Unmanned Aircraft Systems"* [5] recommends the applicable noise evaluation metric depending on the flight operation, *i.e.,* sound exposure level L_{AE} for flyovers and L_{eq} for hovering procedures; both in dB (A).

For a detailed analysis of the noise produced by these novel aircraft, an acoustic characterisation of the sUAS is possible from data post-processing, including back-propagation techniques and noise hemisphere construction [6].

The goal of this paper is to overview a methodology for on-field measurement and analysis of sUAS noise, and report some preliminary results on the feasibility of acoustic characterisation of sUAS during outdoor flyovers.

2. METHODS

The methodological framework for the acoustic characterisation of sUAS is presented in Fig. 1. Acoustic met-

rics can be calculated at each microphone position from multichannel data. Alternatively, Sound Quality Metrics (SQM) are also feasible to calculate from recorded data for psychoacoustic analysis. Then, the acoustic metric based on sound pressure levels are back-propagated at a constant distance r_0. Atmospheric absorption losses, spherical spreading [7], and ground reflection [8] are the main factors included in the back-propagation process. Finally, the directivity of the noise source is constructed with the sound levels back-propagated from each microphone position.

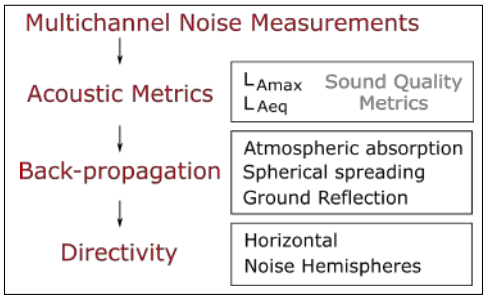

Figure 1. Methodological framework.

2.1 Experimental set-up

The recommendations of the ISO Working Group and NASA-UNWG [9, 10] have been implemented for outdoor tests. A multichannel microphone array simultaneously measures noise at multiple angles along the lateral plane during overflight and hovering operations. As depicted in Fig. 2, the setup considered nine aligned free-field microphones mounted on metal ground plates, in an inverted position at 7 mm from the plate, allocated at constant $\Theta = 15°$ angle resolution.

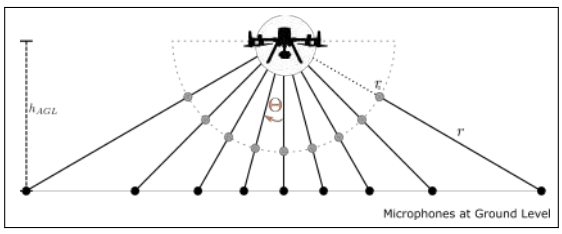

Figure 2. Microphones set-up. r is the distance between the centre of mass of the sUAS and the microphone, and r_0 is the constant distance for sound pressure back-propagation [11].

The environmental conditions were also monitored throughout the measurement period. Air temperature 13-16 $°C$, average wind speeds generally between 0-6$\mathrm{m/s}$ with the predominant wind direction from the southeast. Background noise levels were monitored at periodic intervals throughout the day and measured at a value of approximately $L_{Aeq} = 35\,\mathrm{dB}$ on average.

Two manoeuvres were tested during the measurement campaign. For hovering (reported in [12]), the sUAS operates in a stationary position over the central microphone during $20.0\,\mathrm{s}$. Both operations were carried out at a constant height above the ground $h_{AGL} = 10.0\,\mathrm{m}$. For the flyover operation (reported in this paper), the sUAS describes a transverse trajectory with respect to the microphone line over the central microphone at two airspeeds ($15\,\mathrm{m/s}$, and $5\,\mathrm{m/s}$).

This paper reports the implementation of the proposed measurement and analysis methodology for a series of sUAS flyovers, described in Tab. 1.

Table 1. sUAS Description.

Model	DJI Matrice 300 RTK
Weight [g]	6300
Payload [g]	930
Max Takeoff Weight [g]	9000
Diag. Wheelbase [mm]	895

3. RESULTS

Fig. 3 shows the spectrogram of a corresponding flyover of the DJI Matrice 300 RTK at centre microphone. This spectrogram displays the amplitude and time history of the key deterministic (or tonal) noise components; and also the broadband noise content, mainly present at the time the sUAS overflies the centre microphone.

As shown in Fig. 3, the Blade Passing Frequency (BPF) of each rotor of the sUAS are located in the region of 100 Hz. Interestingly, two of these BPFs seem to interact with each other, resulting in a frequency-modulated amplitude. This might be the reason why Fluctuation Strength has been usually found as correlating with sUAS noise annoyance and perceived loudness [13, 14]

Upper BFP harmonics (*e.g.,* 1st harmonic BPF at 200 Hz) are also clearly visualised in Fig. 3. At high frequencies, the broadband noise component seems to dominate the noise signature, which has been found to be re-

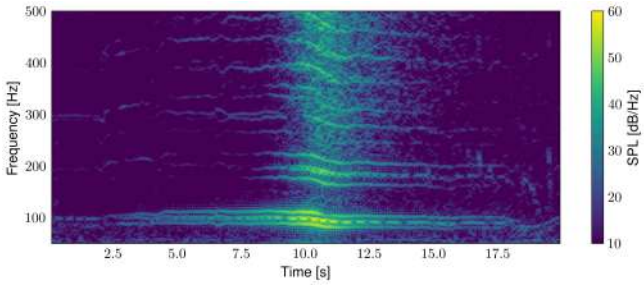

Figure 3. sUAS spectrogram at centre microphone position during downwind flyovers at 10 m h_{AGL} airspeed 15 m/s

lated to the non-deterministic loading noise and turbulence interaction [15].

3.1 Acoustic metrics

The acoustic metric recommended by EASA [5] for sUAS flyover operations is L_{AE}. In this study, the derivation of L_{AE} considers the L_{Aeq} of the flyover event in (1) and (2) whitin the time-window $t'' - t'$ (*i.e.,* when 10 dB drop from the maximum noise level L_{Amax}), where p_0 =20 × 10^{-6} Pa, and t_{ref} =1 s.

$$L_{Aeq} = 10\log_{10}\left(\frac{1}{t''-t'}\int_{t'}^{t''}\frac{p^2_{(t)}}{p_0^2}\,dt\right) \quad (1)$$

$$L_{AE} = L_{Aeq} + 10\log_{10}\left(\frac{t''-t'}{t_{ref}}\right) \quad (2)$$

The L_{AE} of each sUAS flyover event was calculated within the time window highlighted in Fig. 4-a. The power spectral density (PSD) plot in Fig. 4-b illustrates the consistency among the recordings of three consecutive downwind flyovers. It is also possible to observe the BPF tonal components about 100 Hz, the fist harmonic BPF region and the beginning of a dominant broadband region in 500 Hz.

Using the same approach, it is possible to calculate L_{AE} for each microphone position. The results presented in Fig. 4-c describe the symmetry in the reported metrics.

3.2 Directivity

Whereas the acoustic metric is reported on each microphone position, the sound pressure levels are feasible to

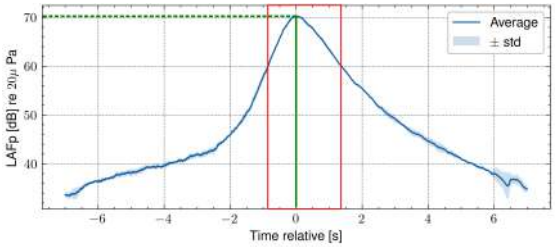

(a) L_{Amax} (green) and time-window for L_{AE} calculation when 10 dBA drop from the maximum level (red) at centre microphone

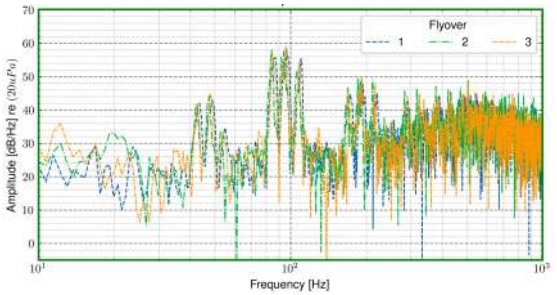

(b) PSDs when L_{max} has been registered at centre microphone

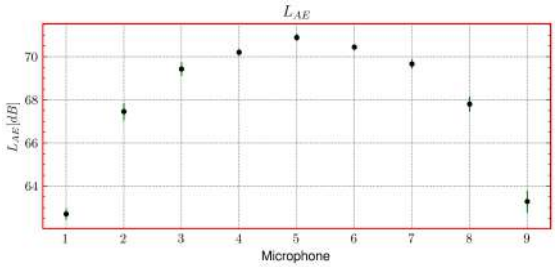

(c) L_{AE} calculated on each microphone position

Figure 4. Noise metrics reported from three downwind consecutive flyovers.

be calculated by means of back-propagation to constant radius around the sUAS.

The horizontal directivity is obtained when the drone emits the flyover's maximum sound pressure level L_{Amax}, approximately when the drone crosses the microphone line. At the same instant, the directivity is feasible to be presented by means of overall sound presure level OASPL or by 1/3 octave bands at angles $-60° \leq \Theta \leq 60°$.

Fig. 5 shows OASPL as directional pattern with high amplitudes underneat the sUAS, whereas the 1/3 octave

band containing the rotors' BPFs shows differences of 3 dB between the two extreme microphone positions. This effect seems to be a consequence of amplitude modulation in the BPF frequency band, which could also have directivity features; however, further research is needed. The broadband noise component in the 1000 Hz band presents two symmetric lobes.

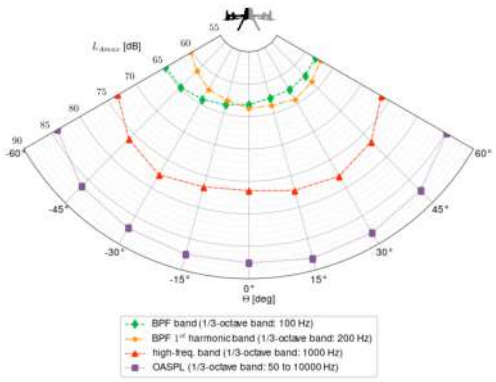

Figure 5. sUAS Directivity at L_{Amax}.

The directivity contours were also calculated in the form of a noise hemisphere representation [6]. First, the horizontal angle was defined by the angle covered $-60° \leq \Theta \leq 60°$ from the position of the microphones. Secondly, the covered polar angle was defined within the time window considered in L_{AE} calculation, $-\phi_{t'}^{\circ} \leq \Phi \leq \phi_{t''}^{\circ}$. By the discretization of this signal segment, the sound levels can be represented by the 1/3 octave band and overall levels.

Fig. 6-a shows the back-propagated amplitude of the 1/3 octave band with the main contribution of the BPF. The modulated amplitude previously detected in the spectrogram (Fig. 3) is also clearly visible in this directivity representation. A similar directivity plot was obtained for the 200 Hz 1/3 octave band; the main contributor is the 1st of BPF Fig. 6-b. The noise hemisphere of 1000 Hz band (including mainly broadband noise) shows two horizontally symmetric lobes as shown in Fig. 5.

Furthermore, the noise hemisphere of the overall sound pressure level (between 50 Hz and 10 000 Hz) also shows that the maximum amplitude of noise emission does not coincide with the position of the drone just above the microphone line. This suggests that the effect that makes the sUAS tilt as it moves forward during the fly-over operation is captured by this directivity plot.

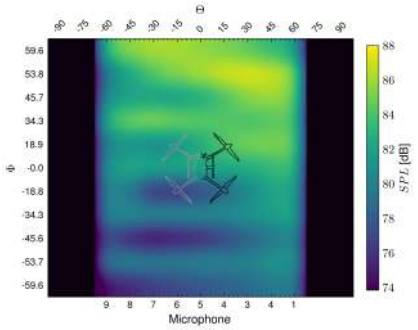

(a) 100 Hz

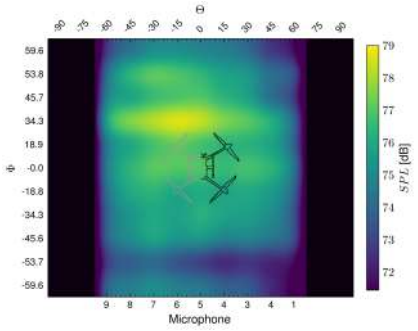

(b) 200 Hz

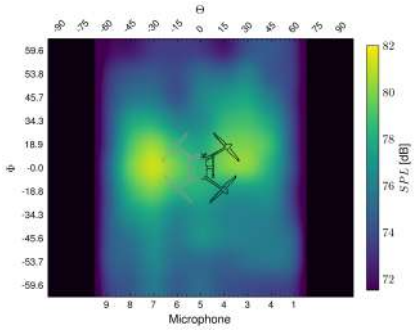

(c) 1000 Hz

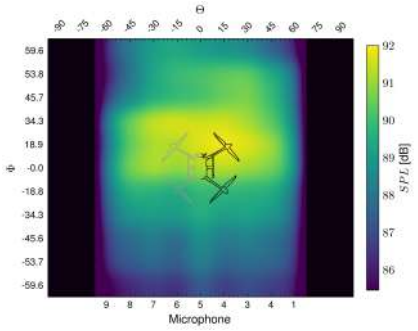

(d) 50 Hz to 10 kHz

Figure 6. 1/3 oct-bands noise hemispheres. (a) BPF-band; (b) BPF 1st harmonic band; (c) High-frequency band; (d) Overall level, from 50 Hz to 10 kHz.

4. CONCLUSSIONS

Currently, there is an effort in developing standardised procedures for sUAS noise measurement using multichannel microphone arrays. This paper presents preliminary results of measurement campaign carried out for a series of sUAS flyovers under very stable and favourable weather conditions (*i.e.,* wind speed lower than $6\,\mathrm{m/s}$)

The method, in compliance with state-of-the-art guidance, allowed the report of acoustic metrics from different microphone positions. In addition, back-propagation of sound pressure levels and the construction of directivity contours allow reporting of noise hemispheres for filtered sound pressure levels per frequency band, overall levels, as well as for a suite of recommended acoustic metrics.

Based on the results obtained for a series of flyovers, the noise signature of the sUAS DJI Matrice 300 RTK is dominated by the noise emitted by the rotors' BPFs at low-mid frecuencies. At high frequencies, the broadband noise component is the one dominating the noise signature of the vehicle under flyover conditions.

Additional GPS tracking data collection would have helped to achieve a more accurate resolution of polar angles during flyovers. Including steps in the signal processing workflow, such as correction of the Doppler effect, were not considered in this paper. However, further work will be carried out for de-Dopplarising acoustic signals, so these data could also be used for auralisation and psychoacoustic testing, *e.g.,* in virtual reality experiments.

While some of the draft procedures being developed have very high requirements for the relative positioning of aircraft and microphones, the results obtained show a good degree of consistency, which may allow the above requirements to be relaxed, making the protocols simpler for certain applications.

5. ACKNOWLEDGMENTS

The authors C.Ramos-Romero, N. Green and A.J. Torija acklowledege the EPSRC-UK funding for DroneNoise project (EP/V031848/1). C. Asensio acknowledges the funding of the "José Castillejo" Mobility Programme from the Ministry of Universities - Spain. All authors wish to acknowledge the support provided by partners DTLX, Edinburgh Drone Company, and Hayes McKenzie Consultants.

6. REFERENCES

[1] T. Zhou, H. Jiang, and B. Huang, "Quad-copter noise measurements under realistic flight conditions," *Aerospace Science and Technology*, vol. 124, p. 107542, 2022.

[2] W. N. Alexander and J. Whelchel, "Flyover noise of multi-rotor suas," in *Inter-Noise and Noise-Con Congress and Conference Proc.*, no. 7, pp. 2548–2558, Institute of Noise Control Engineering, 2019.

[3] N. Kloet, S. Watkins, and R. Clothier, "Acoustic signature measurement of small multi-rotor unmanned aircraft systems," *International Journal of Micro Air Vehicles*, vol. 9, no. 1, pp. 3–14, 2017.

[4] ICAO, "Annex 16 to the Convention on International Civil Aviation. International Standards and Recommended Practices. Environmental Protection. Aircraft Noise," 2017.

[5] EASA, "Guidelines on Noise Measurement of Unmanned Aircraft Systems Lighter than 600 kg. Operating in the Specific Category (Low and Medium Risk). Public Consultation," 2022.

[6] C. M. Hobbs, J. Page, and T. Schultz, "Acoustic re-propagation technique and practical source characterization for simulation noise model databases," in *24th National Conf. on Noise Control Engineering 2010, Noise-Con 2010, Held Jointly with the 159th Meeting of the Acoustical Society of America*, pp. 1166–1178, 2010.

[7] ISO 9613-2:1996, "Acoustics – Attenuationof sound during propagation outdoors – Part 2: General method of calculation," standard, International Organization for Standardization, Geneva, Switzerland, 1996.

[8] P. Rasmussen and L. Lars Winberg, "Accurate measurement of drone noise on the ground," in *QUIET DRONES Second International Symp. on noise from UASs/UAVs and eVTOLs, Paris, France*, p. 11, 2022. INCEEurope, Centre d'information sur le Bruit.

[9] ISO/TC 20/SC 16, "Unmanned aircraft systems," technical committee, American National Standards Institute, Washington 20036 DC, USA, 2022.

[10] NASA-UNWG-Subgroup 2, "UAM Ground & Flight Test Measurement Protocol," 2022. Accessed: 2022-04-11.

[11] N. Green, C. Ramos-Romero, and A. Torija-Martinez, "Advances in the measurement and human response to noise of unmanned aircraft systems," in *INTER-NOISE and NOISE-CON Congress and Conference Proceedings*, vol. 266, pp. 808–817, Institute of Noise Control Engineering, 2023.

[12] C. Ramos-Romero, N. Green, C. Asensio, and A. J. Torija, "sUAS Noise Characterisation During Hovering Operations," in *10th Convention of the European Acoustic Asociation - Forum Acusticum 2023 Proc.*, Italian Acoustical Association, 2023.

[13] D. Y. Gwak, D. Han, and S. Lee, "Sound quality factors influencing annoyance from hovering UAV," *Journal of Sound and Vibration*, vol. 489, p. 115651, 2020.

[14] A. J. Torija and R. K. Nicholls, "Investigation of metrics for assessing human response to drone noise," *International Journal of Environmental Research and Public Health*, vol. 19, no. 6, p. 3152, 2022.

[15] B. Schäffer, R. Pieren, K. Heutschi, J. M. Wunderli, and S. Becker, "Drone noise emission characteristics and noise effects on humans—a systematic review," *International Journal of Environmental Research and Public Health*, vol. 18, no. 11, p. 5940, 2021.